

A Dual Quadrupole Trap for Molecular Spin-Flip Loss

David Reens, Hao Wu, Tim Langen, and Jun Ye
Physics Department, University of Colorado at Boulder

(Dated: March 7, 2017)

A new electromagnetic trap geometry allows full tuning of complex molecular spin-dynamics in crossed electric and magnetic fields. If not tuned properly, these dynamics lead to spin-flip loss that afflicts a wide set of candidate molecules. The spin-flip loss can be significant even above 100 mK and increases with $1/T$, so its removal represents a critical step toward ultracold molecules. The trapping geometry features a 0.5 K trap depth and 5 T/cm trap strength, and allows spin-dynamics to be tuned with only an external bias coil. Spin-flip loss is tuned in a 170 mK sample of OH molecules from over 200 s $^{-1}$ to below the vacuum limited lifetime of 2 s $^{-1}$.

The ultracold regime extends toward molecules on many fronts [1]. Several bialkali molecules are available [2–4] and others are under development. Creative and carefully engineered laser cooling strategies are tackling certain nearly vibrationally diagonal molecules [5–9]. A plethora of non-optical cooling strategies have succeeded to greater or lesser extents on other molecules [10–14]. All of these molecules will require secondary strategies like evaporation or sympathetic cooling to make further gains in phase space density. They also may face a familiar challenge: spin flip loss near the zero of a magnetic trap, but dramatically enhanced for many doubly dipolar molecules due to their internal spin dynamics in mixed electric and magnetic fields.

The knowledge of spin flips or Majorana hops as an eventual trap lifetime limit predates the very first magnetic trapping of neutrals [15]. Spin flips were directly observed near 10 μ K and overcome in the TOP trap [16], and soon later with a plugged dipole trap [17], famously enabling the first Bose-Einstein condensates. We have previously observed spin-flips in a 45 mK OH sample, more than three orders of magnitude higher in temperature compared with the atomic case. The observation was discussed briefly in the appendix of [18]. This loss occurred in a 3D permanent magnet quadrupole trap, first introduced in [19], with a superposed homogeneous electric field. We will use this geometry, detailed in panels (d) and (e) of fig. 1, as our starting point to explain the internal spin-dynamics that lead to this spin-flip loss. We then explain our new trapping geometry and how it achieves tunable removal of spin-flip loss. The internal spin-dynamics are applicable to Hund's case A molecules and to Hund's case B molecules to a lesser extent.

The internal spin-dynamics that lead to this enhanced spin-flip loss are subtle, having eluded two previous investigations. In [21] the analogues of atomic spin-flip loss for molecules in mixed fields were investigated, and our focus case, a magnetic quadrupole trap for OH molecules with superposed electric field, was specifically addressed. It was concluded that no significant loss enhancement due to electric field should be evident. While this is true for the approximate $^2\Pi_{1/2}$ Hamiltonian used in that study,

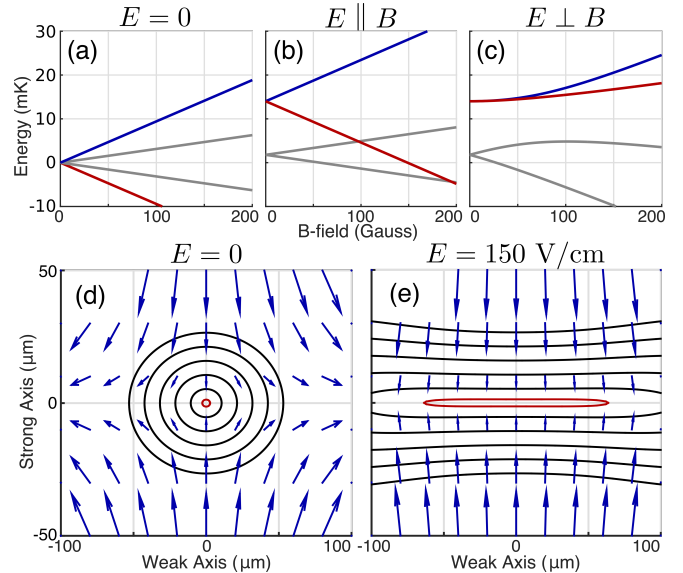


FIG. 1. The blocking effect. (a), four Zeeman split lines in OH's $J = 3/2$ ground manifold. A nearly identical set of opposite parity lie 1.7 GHz below. The trapped state (blue) and its spin-flip partner (red). (b) Zeeman splitting, $E \parallel B$, $E = 150$ V/cm. (c) $E \perp B$. Note vastly reduced red-blue splitting. See all angles in appendix of [18]. (d) Energy splitting contours every 2 mK near the zero of our 2 T/cm trap [20]. B-field arrows in blue. (e) Again with $E = 150$ V/cm. Note drastic widening of lowest contour (red). Vector direction gives the Hund's Case X quantization axis of trapped state, $\mu_B B \pm d_E E$ above (below) the center plane. Vector magnitude gives potential energy relative to trap center.

it is not true for the actual $^2\Pi_{3/2}$ ground state of OH. In [22], it was correctly noted that Hund's case A molecules maintain a quantization axis in mixed fields. In fact the various ground states of the molecule align with one of two quantization axes- either the vector sum or the vector difference of the dipole moment weighted electric and magnetic fields. It was asserted that this would maintain quantization near the zero of a quadrupole trap and avoid spin-flip loss. Quantization is maintained, but this does not hinder but rather aids the spin-flip loss.

This is the crux of the internal spin-dynamics that lead

to loss. With only magnetic field, a molecule remains trapped insofar as it adiabatically follows the field direction. Near the trap center, the direction changes most rapidly, enabling loss. When electric field is added, it dominates in the trap center where the magnetic field is weakest. Quantization is maintained but the quantization axis does not rotate with the magnetic field as it needs to. Further away from the trap center the molecule is then magnetically strong field seeking and is lost. The molecule ought to have switched from the vector sum quantization axis to the vector difference quantization axis, so as to remain doubly weak field seeking despite the change in relative orientation of the fields. [23]

In terms of energies, this manifests as an unusually narrow Zeeman splitting in the region where the relative field orientation changes, i.e. where the fields are orthogonal. In our focus case this occurs in a plane through the trap center, but generally it is always a 2D region since it is a level set of the continuous scalar $\phi = E \cdot B$. In the subset of the plane where $\mu_B B \ll d_E E$, the Zeeman effect is not linear but cubic. We call this “blocking”, see fig. 1, and we say that the E-field blocks the Zeeman effect from linear to cubic. Eventually the Zeeman effect overcomes the blocking and returns to linear when $d_E E \approx \mu_B B$. The Stark effect is not blocked by the Zeeman thanks to lambda doubling, which gives a large fixed energy barrier between opposite alignment with the electric field.

This observation allows us to develop a scaling law for the enhancement. For a given trap strength and sample temperature, there is a characteristic energy splitting κ below which spin-flips can occur, calculated from the Landau-Zener formula. In our case $\kappa = 5$ MHz. As shown in panel (e) of fig. 1, E-field widens the κ valued energy contour near the trap zero, greatly increasing the flux through this region. We can series expand the exact eigenenergies of OH to find $H_{E\perp B}(B) \approx (\mu_B B)^3 \Delta^2 / (d_E E)^4$, Δ the lambda doubling term. Solving for B when $H_{E\perp B} = \kappa$ and dividing by the $E = 0$ case gives the flux enhancement factor $\nu = (d_E E / \sqrt{\kappa \Delta})^{8/3}$. E-fields beyond $\sqrt{\kappa \Delta}$ lead to almost cubic enhancements in spin-flip loss. For other Hund’s case A molecules, similar expressions can be derived. The order of the blocked Zeeman effect is $2J$, so that only $J = 1/2$ molecules are immune, but these are not magnetically trappable due to their vanishing g-factor. For Hund’s case B the enhanced loss region is restricted to the trap energy regime where γ the spin-rotation coupling dominates. This can still be significant, for example $\gamma = 75$ MHz for SrF [24].

We can be more quantitative by numerically integrating the velocity distribution and the flux through the plane, accounting for the velocity dependent Landau-Zener probability, see Table I. The spin-dynamical effect is negligible at initial temperatures, but relevant at the final temperatures targeted during evaporation.[26] With the goal of much colder temperatures than 5 mK,

TABLE I. Enhancements and loss rates for OH. Evaporation E-field detailed in [25]. Spectroscopic E-field in [20]. Background loss is 2 s^{-1} , experiment length 100 ms.

E field	45 mK		5 mK		Purpose
	ν	$\Gamma(s^{-1})$	ν	$\Gamma(s^{-1})$	
0 V/cm	1	0.02	1	1.3	No Field
300 V/cm	5	0.1	9	11	Evaporation
550 V/cm	17	0.3	40	50	Spectroscopy
3 kV/cm	1000	19	1600	2000	Polarizing

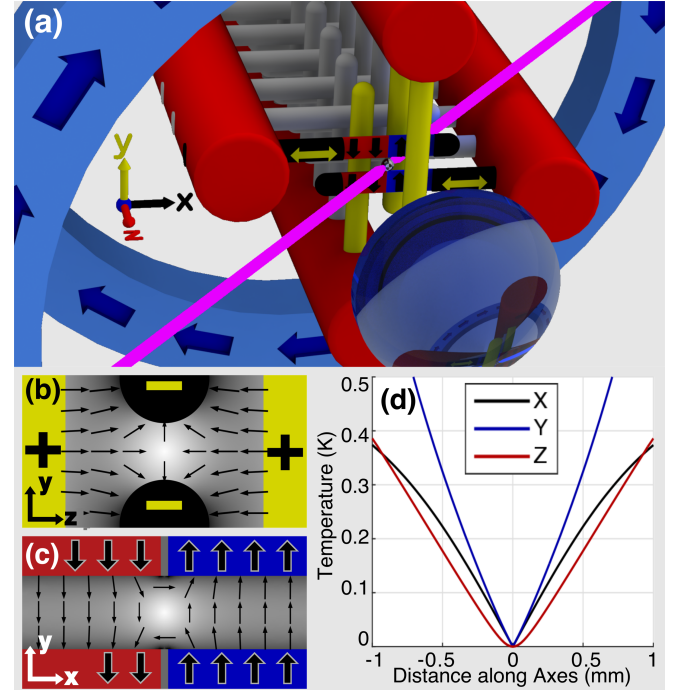


FIG. 2. Panel (a). Dual quadrupole trap embedded in Stark Decelerator. The decelerator has four backbone electrodes (red) and many pin electrodes (gray). OH produced and slowed as in [19], except the slowing extends nearly to zero velocity between the second to last pin pair (black), magnetized as detailed in panel (c). Four pins then form the electric trapping quadrupole (yellow, one omitted for clarity), the last and third to last pin pairs. Detail in panel (b). Trapping pins are conductive with decelerator backbone; voltage configurations achieved with existing feedthroughs but modified MOSFET setup for bipolar output. Yellow bidirectional arrows indicate translations described in the text. Bias coils (light blue) and their current direction (dark blue) sit outside vacuum. LIF detection with laser (pink) and collection lens (blue). Panel (d) shows trap energy along axes. $B' = 5 \text{ T/cm}^2$ and $E' = 100 \text{ kV/cm}^2$. Trap frequencies $\nu_x = 3 \text{ kHz}$, $\nu_y = 5 \text{ kHz}$, and $\nu_z = 4 \text{ kHz}$.

it is clear that the spin-flip loss must be addressed.

We can sum up with a simple strategy: avoid $\mu_B B < d_E E$ where $E \perp B$. One way to obey this is to trap with E-field and superpose B-field. Although the lambda doublet prevents flips in this configuration, it also weakens the trap considerably, undesirable for maintaining large

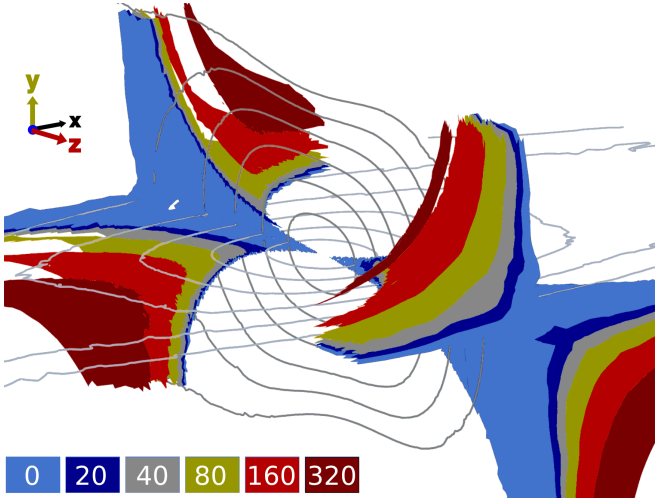


FIG. 3. Each color shows the surfaces where spin-flip can occur for the particular value of B_{coil} given by the legend in units of Gauss. Trap energy contours are shown in gray. Larger B_{coil} pushes the loss regions away from the trap center.

trap frequencies at low temperatures. Another option is to trap with both fields and keep zeros overlapped. This prevents spin-flip loss enhancement, but does not remove it entirely. It is also susceptible to misalignment induced spin-flip loss. A superposed magnetic quadrupole and electric hexapole has been realized for OH [27]. Although the use of only a single field would avoid spin-flip loss, any experiment which aims to make use of the doubly dipolar nature of molecules cannot accept this compromise.

Seeking to remove the loss entirely but without trap depth or trap gradient sacrifice, we use a pair of 2D quadrupole traps, one magnetic and the other electric, with orthogonal axes. We achieve these fields with a geometry that matches our Stark decelerator [13], as shown in fig. 2. This approach is similar to the Ioffe-Pritchard strategy [28], where a 2D quadrupole is combined with an axial dipole trap. Axial and radial trapping interfere, resulting in significantly lower trap depths than the 3D quadrupole. We thwart this interference by using electric field for the third direction. This geometry has $E \perp B$ along both the $x - z$ and $y - z$ planes, with $\mu_B B < d_E E$ in a large cylinder surrounding the z -axis. However, by adding magnetic field along the zero axis of the magnetic quadrupole with external bias coils, a fully tunable scenario emerges.

B_{coil} allows a full tuning from the fast 200 s^{-1} loss trace recorded in Panel (b) of Fig. 4 to complete removal. It does this by morphing the $E \perp B$ surface from a pair of planes into a hyperbolic sheet which deviates spatially from the magnetic field minimum along the z -axis. Thanks to this deviation, for suitable magnitude of B_{coil} , $\mu_B B < d_E E$ can be avoided. In fig. 3, the surfaces where $B \perp E$ are colored wherever the splitting there is

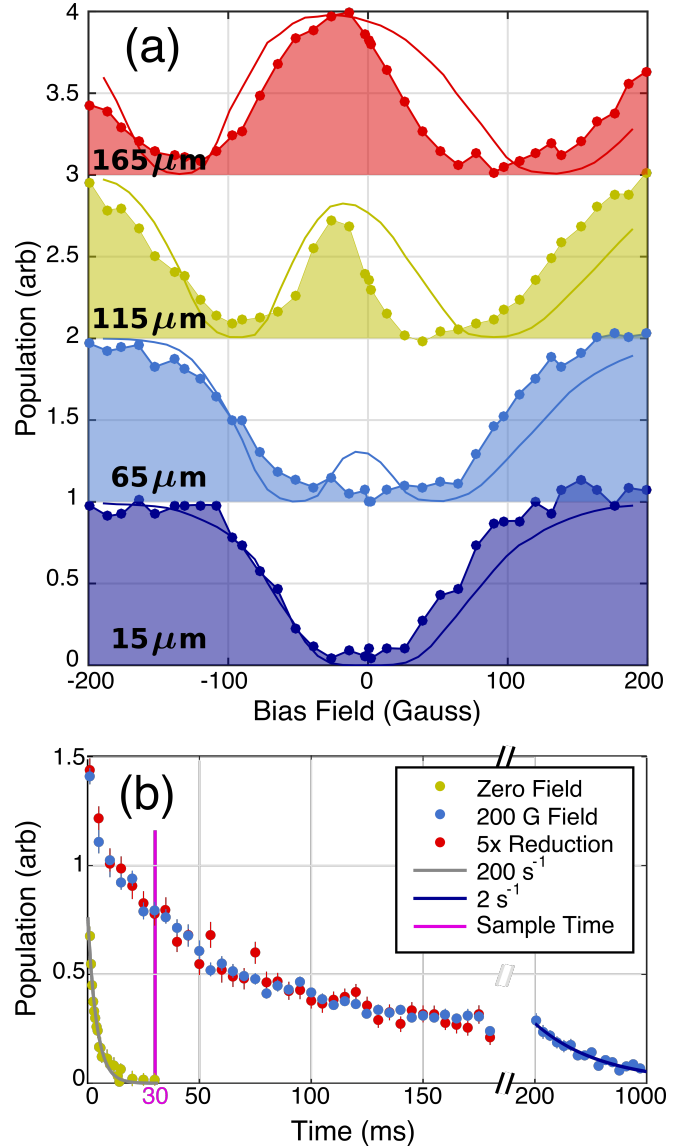


FIG. 4. Panel (a). Family of curves showing the population after 30ms as a function of pin translation and bias field. Panel (b). Time traces for aligned pins at two bias fields, a density modulated trace, and an extended time trace.

below the hopping threshold κ . Note how B_{coil} tunes the proximity of the loss regions to zero. The loss regions are always visible, but they are tuned so far from the trap center that molecules accessing them have already escaped the trap.

As a further confirmation of our $E \perp B$ and $\mu_B B < d_E E$ model of the loss, we translate our magnetic pins in their mounts to alter the surface where $E \perp B$ and compare experimental data against our expectations. The data are shown in fig. 4. Qualitatively, this translation serves to disrupt the otherwise perfectly 2D magnetic quadrupole by adding a small trapping field $\vec{B} \propto B' z \hat{z}$ along the z -axis. This means that B_{coil} no longer directly tunes the minimum magnetic field in the trap. Instead,

B_{coil} must first overcome the slight trapping field along the z -axis, translating a point of zero field along the z axis and eventually out of the trap. The point of zero field disrupts the previously hyperbolic $E \perp B$ surface, causing it to twist and intersect the z -axis near the magnetic zero. This intersection point has $\mu_B B \ll d_E E$ except when aligned with the trap center, where E also goes to zero. This means that without any bias field, the loss should actually be a local minimum; as the field is increased in either direction the loss should first worsen and then improve when the zero leaves the trap. This qualitative explanation correctly predicts the observed double well structure.

Quantitatively, we fit the family of curves shown in fig. 4 by performing an integration of molecule flux weighted by Landau-Zener probability and Maxwell-Boltzmann population density over the strangely twisted hyperbola of $E \perp B$. The computation is performed in COMSOL Multiphysics, accounting for the expected magnetic and electric fields from the trapping geometry with various offsets and with cloud temperature as the only free parameter.[29] The fit temperature is approximately 170 mK. The asymmetry of the curves about the $B_{\text{coil}} = 0$ axis comes from a slight shift of the electric quadrupole minimum caused by an intentional bending of the last pin pair to increase fluorescence collection. This offset is not a free parameter in the model, it is directly included according to the measured bending applied to the pins. The fitted temperature is larger than expected from our simulations of the geometry, despite the known defocusing and reflection losses that accompany pulsed decelerators at low speeds [30]. This may be related to micro-discharges on the surfaces of the magnetic pins during the final deceleration pulse. The magnetic pins are not currently polished as well as the rest of the decelerator, but this is not a fundamental limitation and could be overcome by diamond turning of the nickel plating on the pins or some other polishing strategy.

Another way to validate our understanding of molecular spin-flip loss in our dual quadrupole trap would be to confirm that the location of the loss is indeed tuned away from the trap center with increasing B_{coil} as shown in fig. 3. We achieve this with a Zeeman microwave spectroscopy performed as in our previous work [25]. Rather than using a bias tee setup, a challenging prospect with our trap deeply integrated in the high voltage decelerator, we use a microwave probe to directly excite free space cavity modes of our vacuum chamber. The results are shown in fig. 5. With the magnetic pins aligned, it is seen that higher values of B_{coil} indeed increases the population of molecules able to survive at higher fields. In order to perform this spectroscopy, the trapping electric fields are switched off immediately prior to the application of a microwave transfer pulse tuned to a particular magnetic field strength. Thus the results reflect the Zeeman potential energy only, and only loosely correspond to

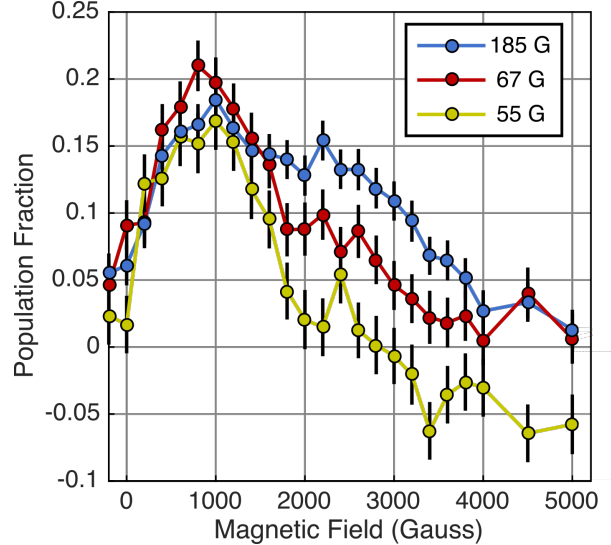


FIG. 5. Microwave Thermometry. Bias field tunes the proximity of loss to the trap center.

the total potential energy of the molecules. Nonetheless, the shift in population center is clear and in agreement with our expectation.

In the case of lowest applied magnetic field in fig. 5, i.e. deepest cutting of the loss region toward the trap center, a negative going signal is observed. This indicates a build-up in the opposite parity weak electric field seeking state. Although the spin-flips we have discussed connect strong and weak field seeking magnetic states, other avoided crossings amongst the ground state manifold result in the spin-flipped molecules remaining partially trapped in a secondary state with a nonuniform gradient (repulsive in the center, attractive outside) and a much lower overall trap depth. This secondary state also exhibits spin-flip loss to other lower states, but the enhancement with electric field is related to a quadratic blocking of the Zeeman splitting, and is thus not as dominating as the loss in the primary state due to cubic blocking.

Once the loss is fully removed, we observe the trend in blue on panel (b) of fig. 4. The decay rate decreases with population over a timescale that is long compared with trap frequency and is thus suggestive of a collisional process. However, a completely phase-space blind density reduction technique [31] that significantly reduces our molecule number causes little change in the shape of the trend, indicating that single-particle physics is responsible. This is attributable to our warmer initial temperature than in previous experiments. The slowly decaying trend could be related to the existence of high energy chaotic orbits with long escape times, as seen in other exotically shaped trapping potentials [32]. We hope in the near future to implement an increase in molecule number rather than a decrease, by means of a suite of

density enhancing experimental improvements.

Our dual quadrupole trap decisively overcomes molecule enhanced spin-flip loss by tuning it from an overwhelming rate to complete removal. Our explanation of the loss provides detailed predictions of how its location and magnitude ought to scale with bias field and trap alignment, which we have experimentally verified. Our results contradict existing predictions about molecular spin-flips in mixed fields and we provide a consistent framework that explains this based on internal spin-dynamics. We have devised a viable trapping geometry in which spin-flip loss is fully mitigated without trap-depth sacrifice, paving the way toward further improvements in molecule trapping and cooling.

-
- [1] L. D. Carr, D. DeMille, R. V. Krems, and J. Ye, *New Journal of Physics* **11**, 055049 (2009).
- [2] K.-K. Ni, S. Ospelkaus, M. H. G. de Miranda, A. Pe'er, B. Neyenhuis, J. J. Zirbel, S. Kotochigova, P. S. Julienne, D. S. Jin, and J. Ye, *Science* **322**, 231 (2008).
- [3] T. Takekoshi, L. Reichsöllner, A. Schindewolf, J. M. Hutson, C. R. Le Sueur, O. Dulieu, F. Ferlaino, R. Grimm, and H.-C. Nägerl, *Physical Review Letters* **113**, 205301 (2014).
- [4] J. W. Park, S. A. Will, and M. W. Zwierlein, *Physical Review Letters* **114**, 205302 (2015).
- [5] M. H. Steinecker, D. J. McCarron, Y. Zhu, and D. DeMille, *ChemPhysChem* **17**, 3664 (2016).
- [6] J. F. Barry, D. J. McCarron, E. B. Norrgard, M. H. Steinecker, and D. DeMille, *Nature* **512**, 286 (2014).
- [7] B. Hemmerling, E. Chae, A. Ravi, L. Anderegg, G. K. Drayna, N. R. Hutzler, A. L. Collopy, J. Ye, W. Ketterle, and J. M. Doyle, *Journal of Physics B: Atomic, Molecular and Optical Physics* **49**, 174001 (2016).
- [8] M. T. Hummon, M. Yeo, B. K. Stuhl, A. L. Collopy, Y. Xia, and J. Ye, *Physical Review Letters* **110**, 143001 (2013).
- [9] V. Zhelyazkova, A. Cournoil, T. E. Wall, A. Matsushima, J. J. Hudson, E. A. Hinds, M. R. Tarbutt, and B. E. Sauer, *Physical Review A* **89**, 053416 (2014).
- [10] J. M. Doyle, J. D. Weinstein, R. DeCarvalho, T. Guillet, and B. Friedrich, *Nature* **395**, 148 (1998).
- [11] A. Prehn, M. Ibrügger, R. Glöckner, G. Rempe, and M. Zeppenfeld, *Physical Review Letters* **116**, 063005 (2016).
- [12] H. L. Bethlem, G. Berden, and G. Meijer, *Physical Review Letters* **83**, 1558 (1999).
- [13] J. R. Bochinski, E. R. Hudson, H. J. Lewandowski, G. Meijer, and J. Ye, *Physical Review Letters* **91**, 243001 (2003).
- [14] N. Akerman, M. Karpov, L. David, E. Lavert-Ofir, J. Narevicius, and E. Narevicius, *New Journal of Physics* **17**, 065015 (2015).
- [15] A. L. Migdall, J. V. Prodan, W. D. Phillips, T. H. Bergeman, and H. J. Metcalf, *Physical Review Letters* **54**, 2596 (1985).
- [16] W. Petrich, M. H. Anderson, J. R. Ensher, and E. A. Cornell, *Physical Review Letters* **74**, 3352 (1995).
- [17] K. B. Davis, M. O. Mewes, M. R. Andrews, N. J. van Druten, D. S. Durfee, D. M. Kurn, and W. Ketterle, *Physical Review Letters* **75**, 3969 (1995).
- [18] B. K. Stuhl, M. Yeo, M. T. Hummon, and J. Ye, *Molecular Physics* **111**, 1798 (2013).
- [19] B. C. Sawyer, B. K. Stuhl, D. Wang, M. Yeo, and J. Ye, *Physical Review Letters* **101**, 203203 (2008).
- [20] B. K. Stuhl, M. Yeo, B. C. Sawyer, M. T. Hummon, and J. Ye, *Physical Review A* **85**, 033427 (2012).
- [21] M. Lara, B. L. Lev, and J. L. Bohn, *Physical Review A* **78**, 033433 (2008).
- [22] J. L. Bohn and G. Quéméner, *Molecular Physics* **111**, 1931 (2013).
- [23] In fact, the only reason a molecule can remain trapped at all in this configuration is thanks to the lambda doubling perturbation, which connects the substates of different quantization axes and creates a barrier to remaining in the same quantization axis. In a hypothetical perfectly linear Stark effect molecule without this doubling, an arbitrarily small stray electric field would cause complete trap loss for molecules crossing the center plane of the trap.
- [24] G. Quéméner and J. L. Bohn, *Physical Review A - Atomic, Molecular, and Optical Physics* **93**, 1 (2016).
- [25] B. K. Stuhl, M. T. Hummon, M. Yeo, G. Quéméner, J. L. Bohn, and J. Ye, *Nature* **492**, 396 (2012).
- [26] For this and other reasons, it is evident that 5 mK temperatures were not actually attained. However it does seem that some phase space compression was achieved for 20 mK evaporation.
- [27] B. C. Sawyer, B. L. Lev, E. R. Hudson, B. K. Stuhl, M. Lara, J. L. Bohn, and J. Ye, *Physical Review Letters* **98**, 1 (2007).
- [28] D. E. Pritchard, *Physical Review Letters* **51**, 1336 (1983).
- [29] Soure code is available: <https://github.com/dreens/spin-flip-integration/>.
- [30] B. C. Sawyer, B. K. Stuhl, B. L. Lev, J. Ye, and E. R. Hudson, *European Physical Journal D* **48**, 197 (2008).
- [31] Microwaves applied via our free space cavity mode probe couple electrically weak and strong field seeking states during deceleration. The microwave wavelength of 15 cm is large compared with packet size, and the resonant energy corresponds to the low electric fields that all molecules experience when flying between stages.
- [32] R. González-Férez, M. Iñarrea, J. P. Salas, and P. Schmelcher, *Physical Review E* **90**, 062919 (2014).
- [33] M. Zeppenfeld, B. G. U. Englert, R. Glöckner, A. Prehn, M. Mielenz, C. Sommer, L. D. van Buuren, M. Motsch, and G. Rempe, *Nature* **491**, 570 (2012).
- [34] I. I. Rabi, *Physical Review* **49**, 324 (1936).
- [35] T. H. Bergeman, P. McNicholl, J. Kycia, H. Metcalf, and N. L. Balazs, *Journal of the Optical Society of America B* **6**, 2249 (1989).
- [36] R. Golub and J. M. Pendleton, *Reports on Progress in Physics* **42**, 439 (1979).